AAC Journals.ASM.org

Antiviral Potential of ERK/MAPK and PI3K/AKT/mTOR Signaling Modulation for Middle East Respiratory Syndrome Coronavirus Infection as Identified by Temporal Kinome Analysis

Jason Kindrachuk,[a] Britini Ork,[a] Brit J. Hart,[a] Steven Mazur,[a] Michael R. Holbrook,[a] Matthew B. Frieman,[b] Dawn Traynor,[a] Reed F. Johnson,[c] Julie Dyall,[a] Jens H. Kuhn,[a] Gene G. Olinger,[a] Lisa E. Hensley,[a] Peter B. Jahrling[a,c]

Integrated Research Facility, National Institute of Allergy and Infectious Diseases, National Institutes of Health, Frederick, Maryland, USA[a]; Department of Microbiology and Immunology, University of Maryland at Baltimore, Baltimore, Maryland, USA[b]; Emerging Viral Pathogens Section, National Institute of Allergy and Infectious Diseases, National Institutes of Health, Frederick, Maryland, USA[c]

Middle East respiratory syndrome coronavirus (MERS-CoV) is a lineage C betacoronavirus, and infections with this virus can result in acute respiratory syndrome with renal failure. Globally, MERS-CoV has been responsible for 877 laboratory-confirmed infections, including 317 deaths, since September 2012. As there is a paucity of information regarding the molecular pathogenesis associated with this virus or the identities of novel antiviral drug targets, we performed temporal kinome analysis on human hepatocytes infected with the Erasmus isolate of MERS-CoV with peptide kinome arrays. bioinformatics analysis of our kinome data, including pathway overrepresentation analysis (ORA) and functional network analysis, suggested that extracellular signal-regulated kinase (ERK)/mitogen-activated protein kinase (MAPK) and phosphoinositol 3-kinase (PI3K)/serine-threonine kinase (AKT)/mammalian target of rapamycin (mTOR) signaling responses were specifically modulated in response to MERS-CoV infection *in vitro* throughout the course of infection. The overrepresentation of specific intermediates within these pathways determined by pathway and functional network analysis of our kinome data correlated with similar patterns of phosphorylation determined through Western blot array analysis. In addition, analysis of the effects of specific kinase inhibitors on MERS-CoV infection in tissue culture models confirmed these cellular response observations. Further, we have demonstrated that a subset of licensed kinase inhibitors targeting the ERK/MAPK and PI3K/AKT/mTOR pathways significantly inhibited MERS-CoV replication *in vitro* whether they were added before or after viral infection. Taken together, our data suggest that ERK/MAPK and PI3K/AKT/mTOR signaling responses play important roles in MERS-CoV infection and may represent novel drug targets for therapeutic intervention strategies.

Middle East respiratory syndrome (MERS) is a viral respiratory disease that results from infection with the MERS coronavirus (MERS-CoV) and was first identified in a patient with acute pneumonia and renal failure in Jeddah, Kingdom of Saudi Arabia, in June 2012 (1). Subsequently, there have been 877 laboratory-confirmed MERS-CoV infections to date, including 317 deaths (http://www.who.int/csr/don/16-october-2014-mers/en/), resulting in a case fatality rate of 30%, with all cases directly or indirectly being linked to the Middle East region (2). Recent announcements of laboratory-confirmed cases of MERS-CoV infection in patients in the United States and the Netherlands have further exacerbated concerns regarding the global evolution of this epidemic (3).

MERS-CoV belongs to the same genus (*Betacoronavirus*) as severe acute respiratory syndrome (SARS) coronavirus (SARS-CoV), which was responsible for the global SARS pandemic of 2002 and 2003 that affected more than 8,000 people (4), and the human coronaviruses (HCoVs) HKU1 and OC43, which cause mild to moderate respiratory disease (5). Further, MERS-CoV is the first lineage 2c betacoronavirus shown to infect humans (6, 7). Although the natural reservoir for MERS-CoV has yet to be determined, it has been suggested that bats are a likely candidate, given the similarity of MERS-CoV to bat coronaviruses (8). Recent evidence has also suggested that dromedary camels may act as an intermediate host for MERS-CoV, as supported by serological, genetic, and epidemiological evidence as well as the recent isolation of the virus (9, 10). Animal-to-human transmission has largely been suspected to be the primary contributor to the recent outbreaks of MERS-CoV. Although human-to-human transmission has been reported in several case clusters, there is currently no evidence for sustained community transmission (11). MERS-CoV infections have been associated with severe lower respiratory tract infections, including acute respiratory syndrome with renal failure. Interestingly, the severity of disease presentation appears to be related to underlying comorbidities, as MERS-CoV infections in healthy individuals appear to result primarily in mild to asymptomatic disease (1, 12, 13).

Though appreciable efforts have been made to identify novel

Received 17 June 2014 **Returned for modification** 22 July 2014
Accepted 29 October 2014

Accepted manuscript posted online 8 December 2014

Citation Kindrachuk J, Ork B, Hart BJ, Mazur S, Holbrook MR, Frieman MB, Traynor D, Johnson RF, Dyall J, Kuhn JH, Olinger GG, Hensley LE, Jahrling PB. 2015. Antiviral potential of ERK/MAPK and PI3K/AKT/mTOR signaling modulation for Middle East respiratory syndrome coronavirus infection as identified by temporal kinome analysis. Antimicrob Agents Chemother 59:1088–1099. doi:10.1128/AAC.03659-14.

Address correspondence to Jason Kindrachuk, kindrachuk.kenneth@nih.gov.

Supplemental material for this article may be found at http://dx.doi.org/10.1128/AAC.03659-14.

doi:10.1128/AAC.03659-14

antiviral therapeutics for MERS-CoV, there are currently no approved therapeutic interventions available, and treatment is based on supportive care (14). Initial investigations of interferon (IFN) demonstrated that alpha interferon (IFN-α), IFN-γ, and IFN-β were able to inhibit MERS-CoV replication (15, 16). Subsequent studies demonstrated that among the different interferons, IFN-β had the strongest inhibitory activity against MERS-CoV (17). Mycophenolic acid, IFN-β, and ribavirin have been demonstrated to have strong inhibitory activities against MERS-CoV *in vitro* (17, 18), and Falzarano et al. demonstrated that the administration of IFN-α2b and ribavirin resulted in synergistic antiviral activities both *in vitro* and *in vivo* in rhesus macaques (19). Josset and colleagues employed systems-level gene expression analysis of MERS-CoV infection *in vitro* and identified that IFN-α5 and IFN-β were specifically upregulated by MERS-CoV infection (20).

Surveys of the host response to infection through either genomic or proteomic technologies have previously been employed to characterize microbial pathogenesis and identify novel therapeutic targets (21–24). The incorporation of systems-level analysis to such investigations provides a unique opportunity to identify specific host or pathogen responses that are modulated during the course of infection. A global transcriptome analysis of host responses to MERS-CoV and SARS-CoV infection suggested that MERS-CoV modulated transcriptional changes in the host differently from the way in which SARS-CoV did, although viral replication kinetics were similar for both viruses (20). Subsequent systems-level analysis of the transcriptome data suggested that changes in the host transcriptome in response to either MERS-CoV or SARS-CoV may be related to the activation state of cell signaling networks. Further, the authors demonstrated that the identification of specific cellular intermediates through upstream regulator analysis could be used to predict potential host targets for therapeutic intervention. However, many cellular processes are regulated independently of changes in transcriptional or translational regulation through kinase-mediated modulation of cell signaling networks. Characterization of the activation state of cellular host kinases, or the kinome, provides a mechanism to identify the individual kinases and/or signaling networks that are of central importance to disease progression or resolution. Previously, we demonstrated the utility of species-specific kinome analysis with peptide kinome arrays for characterizing the modulation of host cell signaling networks, including responses to infection (25, 26).

Here, we have characterized the temporal host kinome response of human hepatocytes to infection with MERS-CoV isolate HCoV-EMC/2012 (MERS-CoV) and identified specific cell signaling networks and kinases that are modulated during the course of infection and may represent novel antiviral targets. As it has previously been demonstrated that Huh7 hepatocytes are highly permissive to MERS-CoV (27) and it is postulated that targets found to be overrepresented in our data sets would potentially represent conserved targets across multiple permissive cell types, we have focused on these cells for our analysis. Subsequent systems biology approaches, including pathway overrepresentation analysis (ORA) and functional network analysis (FNA), were used to identify and compare the specific kinome and cell signaling responses that were modulated throughout the course of MERS-CoV infection. Analysis of our kinome data suggested that extracellular signal-regulated kinase (ERK)/mitogen-activated protein kinase (MAPK) and phosphoinositol 3-kinase (PI3K)/serine-threonine kinase (AKT)/mammalian target of rapamycin (mTOR) signaling responses were specifically modulated in response to MERS-CoV infection *in vitro*. The phosphorylation patterns of specific intermediates within these pathways in the kinome array data correlated with the phosphorylation patterns from Western blot dot arrays. In addition, we confirmed these cellular responses through analysis of the effects of inhibition of these pathways or their intermediates on MERS-CoV infection in tissue culture models. Further, we have demonstrated that a subset of the licensed kinase inhibitors targeting the ERK/MAPK and PI3K/AKT/mTOR pathways significantly inhibited MERS-CoV propagation *in vitro* whether they were added before or after viral infection. Taken together, our investigation demonstrates that ERK/MAPK and PI3K/AKT/mTOR signaling responses play a critical role in MERS-CoV pathogenesis and may be potential targets for therapeutic intervention strategies.

MATERIALS AND METHODS

Cells and virus. Huh7 is a hepatocyte-derived epithelial-like cell line, and Huh7 cells were maintained in Dulbecco's minimal essential medium (DMEM; Sigma-Aldrich) supplemented with 10% (vol/vol) heat-inactivated fetal bovine serum (FBS) in a 37°C humidified incubator with 5% (vol/vol) CO_2. MERS-CoV isolate HCoV-EMC/2012 (MERS-CoV), kindly provided by Rocky Mountain Laboratories (NIH/NIAID) and the Viroscience Laboratory, Erasmus Medical Center (Rotterdam, Netherlands), was used for all experiments and propagated as reported previously (28).

Chemical inhibitors. The United States Food and Drug Administration (FDA)-licensed drugs tested (sorafenib, everolimus, dabrafenib, cabozantinib, afatanib, selumetinib, trametinib, and miltefosine) were purchased from Selleck Chemicals. Additional kinase inhibitors tested included AG490, PKC-412, GF109203X, SB203580, wortmannin, Bay 11-7082, GW5074, PP2, and rapamycin (sirolimus), as well as an inhibitor of nitric oxide synthase 2 (NOS2), L-nitro-arginine methyl ester (L-NAME). All were purchased from Enzo Scientific. The inhibitors were reconstituted according to the manufacturers' recommendations in either water or dimethyl sulfoxide (DMSO).

Viral infections for kinome analysis. Huh7 cells were plated in 6-well plates in fresh DMEM supplemented with 2% (vol/vol) FBS and rested for 24 h prior to infection. Cells were infected with MERS-CoV at a multiplicity of infection (MOI) of 0.05 for 1 h at 37°C in 5% CO_2 with periodic rocking. Following incubation, Huh7 cells were washed twice with phosphate-buffered saline (PBS) to remove unbound virus, replenished with fresh DMEM supplemented with 2% (vol/vol) FBS, and incubated at 37°C in 5% CO_2. MERS-CoV-infected and mock-infected cells and cell culture supernatant were harvested at identified time points (1, 6, and 24 h postinfection [p.i.]) for subsequent kinome analysis. Plaque assays were performed on Vero E6 cells as reported previously (17).

Kinome analysis with peptide arrays. The design, construction, and application of peptide arrays were based upon a previously reported protocol (29). Briefly, MERS-CoV-infected and mock-infected Huh7 cells were scraped and pelleted at 1, 6, and 24 h p.i. Following this, the cell supernatants were discarded and the cell pellets were lysed with 100 μl of lysis buffer (20 mM Tris-HCl, pH 7.5, 150 mM NaCl, 1 mM EDTA, 1 mM EGTA, 1% Triton X-100, 2.5 mM sodium pyrophosphate, 1 mM Na_3VO_4, 1 mM NaF, 1 μg/ml leupeptin, 1 μg/ml aprotinin, 1 mM phenylmethylsulfonyl fluoride) and incubated on ice for 10 min, followed by centrifugation to remove cell debris. Cell lysates were transferred to fresh microcentrifuge tubes, and the total protein from the cell lysates was measured using a bicinchoninic acid (BCA) assay (Pierce) to calculate cell lysate volumes to ensure the loading of equal amounts of total protein onto the arrays. Activation mix (50% glycerol, 50 μM ATP, 60 mM $MgCl_2$, 0.05% Brij 35, 0.25 mg/ml bovine serum albumin) was added to the cell lysate fractions, the mixture was spotted onto human kinome arrays (JPT Tech-

nologies), and the arrays were incubated for 2 h at 37°C as described previously (22). The kinome arrays were subsequently washed once with PBS containing 1% Triton X-100, followed by a single wash in deionized H_2O. The peptide arrays were held on dry ice and subjected to gamma irradiation (5 Mrd) to inactivate any residual virus following removal from biocontainment. Kinome arrays were submerged in PRO-Q Diamond phosphoprotein stain (Invitrogen) with gentle agitation in the dark for 1 h. Following staining, the arrays were washed in destain (20% acetonitrile, 50 mM sodium acetate, pH 4.0 [Sigma-Aldrich]) 3 times for 10 min per wash, with the addition of fresh destain each time. A final wash was performed with deionized H_2O, and the arrays were placed in 50-ml conical tubes to air dry for 20 min. The remaining moisture was removed by centrifugation of the arrays at 300 × *g* for 3 min. Array images were acquired using a PowerScanner microarray scanner (Tecan) at 532 to 560 nm with a 580-nm filter to detect dye fluorescence. Images were collected using GenePix (version 6.0) software (MDS). Signal intensity values were collected using GenePix (version 6.0) software (MDS). All data processing and subsequent analysis were performed using Platform for Integrated, Intelligent Kinome Analysis (PIIKA) software (http://saphire.usask.ca/saphire/piika) (29, 30) as described previously (22).

Pathway overrepresentation analysis and functional network analysis. Pathway overrepresentation analysis of differentially phosphorylated proteins was performed using InnateDB software, a publically available resource that predicts biological pathways on the basis of experimental fold change data sets in humans, mice, and bovines (31). Pathways are assigned a probability (*P*) value on the basis of the number of genes present for a particular pathway as well as the degree to which they are differentially expressed or modified relative to their expression under a control condition. For our investigation, input data were limited to peptides that demonstrated consistent responses across the biological replicates ($P < 0.05$) as well as statistically significant changes in expression from that under the control condition ($P < 0.20$), as reported previously (29). Additionally, functional networks were created using Ingenuity Pathway Analysis (IPA) software (Ingenuity Systems, Redwood City, CA). Protein identifiers and the respective phosphorylation fold change values and *P* values were uploaded and mapped to their corresponding protein objects in the IPA knowledge base. Networks of these proteins were algorithmically generated on the basis of their connectivity and assigned a score. Proteins are represented as nodes, and the biological relationship between two nodes is represented as an edge (a solid line for direct relationships and a dotted line for indirect relationships). The intensity of the node color indicates the degree of upregulation (red) or downregulation (green) of phosphorylation. Proteins in uncolored nodes were not identified as being differentially expressed in our experiment and were integrated into the computationally generated networks on the basis of the evidence stored in the IPA knowledge database indicating a relevance to this network.

Western blot array analysis of protein phosphorylation. Huh7 cells were infected with MERS-CoV or mock infected, as described above. Cells from infected or mock-infected cells were harvested at 1, 6, or 24 h p.i., lysed in SDS loading buffer without bromophenol blue (200 mM Tris-HCl, pH 6.8, 8% SDS, 40% glycerol, 4% β-mercaptoethanol, 50 mM EDTA), and boiled for 20 min at 95°C to inactivate remaining virus (as approved within facility-specific standard operating procedures). Following inactivation, supernatants were removed from biocontainment and boiled again for 20 min at 95°C for subsequent analysis. The protein concentration was determined using a BCA protein assay kit (Pierce), according to the manufacturer's instructions. Equal amounts of protein from mock-infected or MERS-CoV-infected samples were loaded onto PathScan intracellular signaling antibody array membranes (Cell Signaling Technologies) and analyzed according to the manufacturer's instructions. Images were acquired using a Syngene G:Box Chemi system (Syngene), and quantification of antibody spot intensities was performed using the ImageJ software suite (32).

Cytotoxicity assays. Kinase inhibitor cytotoxicity was determined using the Cytotox colorimetric assay, which measures the amount of lactate dehydrogenase (LDH; Promega) released from treated cells, following the manufacturer's instructions. Huh7 cells were incubated with each of the drugs for 24 h in a 37°C incubator with 5% CO_2 using the inhibitory concentrations used in the assays below. The cell culture supernatants were then used in the Cytotox 96-well assay, and the adsorbance at 490 nm was read with a M1000 Tecan plate reader.

Cell-based ELISA for analysis of inhibition of MERS-CoV infection by kinase inhibitors. Huh7 cells were plated in black, opaque-bottom 96-well plates and allowed to rest for 24 h prior to infection and treatments. The cells were pretreated for either 1 h prior to infection or 2 h postinfection with kinase inhibitors at final concentrations of 0.1, 1, and 10 μM. The final concentration of DMSO was 0.1% for all experimental conditions. Cells were infected with MERS-CoV at an MOI of 0.05 and allowed to incubate for 48 h at 37°C in 5% CO_2 prior to fixation. After 48 h, the cells were fixed with 10% neutral buffered formalin (NBF) for 30 min, the NBF was changed, and the cells were fixed for an additional 24 h at 4°C to ensure viral inactivation following facility-specific standard operating procedures. Viral inhibition was then determined utilizing a cell-based enzyme-linked immunosorbent assay (ELISA) as described by Hart et al. (17).

Plaque reduction assay for analysis of inhibition of MERS-CoV infection by kinase inhibitors. To determine the antiviral activity of the kinase inhibitors, Huh7 cells were incubated with select kinase inhibitors (10 μM) for 1 h prior to infection with MERS-CoV. Cells were infected with MERS-CoV at an MOI of 0.05 for 1 h at 37°C in 5% CO_2 with periodic rocking. Following incubation, Huh7 cells were washed twice with PBS to remove unbound virus, replenished with fresh DMEM supplemented with 2% (vol/vol) FBS, and incubated at 37°C in 5% CO_2 with or without readministration of the same kinase inhibitor (10 μM). Cell supernatants from the infected and mock-infected cells were harvested 48 h p.i., and the inhibitory activity of the kinase inhibitor-treated cells was assessed by plaque reduction assay as described previously (17).

RESULTS

Temporal kinome analysis of MERS-CoV-infected hepatocytes. To gain insight into potential host signaling networks or kinases that are modulated during MERS-CoV infection and that may represent novel therapeutic targets, we performed temporal kinome analysis of MERS-CoV-infected Huh7 human hepatocytes. Previously, de Wilde et al. demonstrated that Huh7 cells were highly permissive to MERS-CoV infection (27), and we postulated that host signaling networks or individual proteins identified by our analysis may be broadly conserved across multiple cell types targeted by MERS-CoV. In addition, we employed a low multiplicity of infection (MOI = 0.01) to identify host signaling networks or intermediates in an effort to recapitulate circumstances in which host cells would encounter small amounts of virus (i.e., during the initial phases of natural infection). Cells were harvested at multiple time points (1, 6, and 24 h) postinfection (p.i.) alongside time-matched, mock-infected control cells. Kinome analysis with peptide arrays relies on the phosphorylation of specific kinase targets (immobilized peptides) on the arrays by active kinases in a cell lysate (22). Our arrays contained 340 unique peptides representing key phosphorylation events from a broad spectrum of cell signaling pathways and processes. The kinome data were extracted from the arrays and analyzed using the PIIKA software tool (29, 30). Hierarchical clustering analysis demonstrated that the MERS-CoV-infected sample harvested at 1 h p.i. clustered between the mock-infected samples, whereas the MERS-CoV samples harvested at 6 h and 24 h p.i. clustered outside the mock-infected samples, suggesting an increased diversity in the host

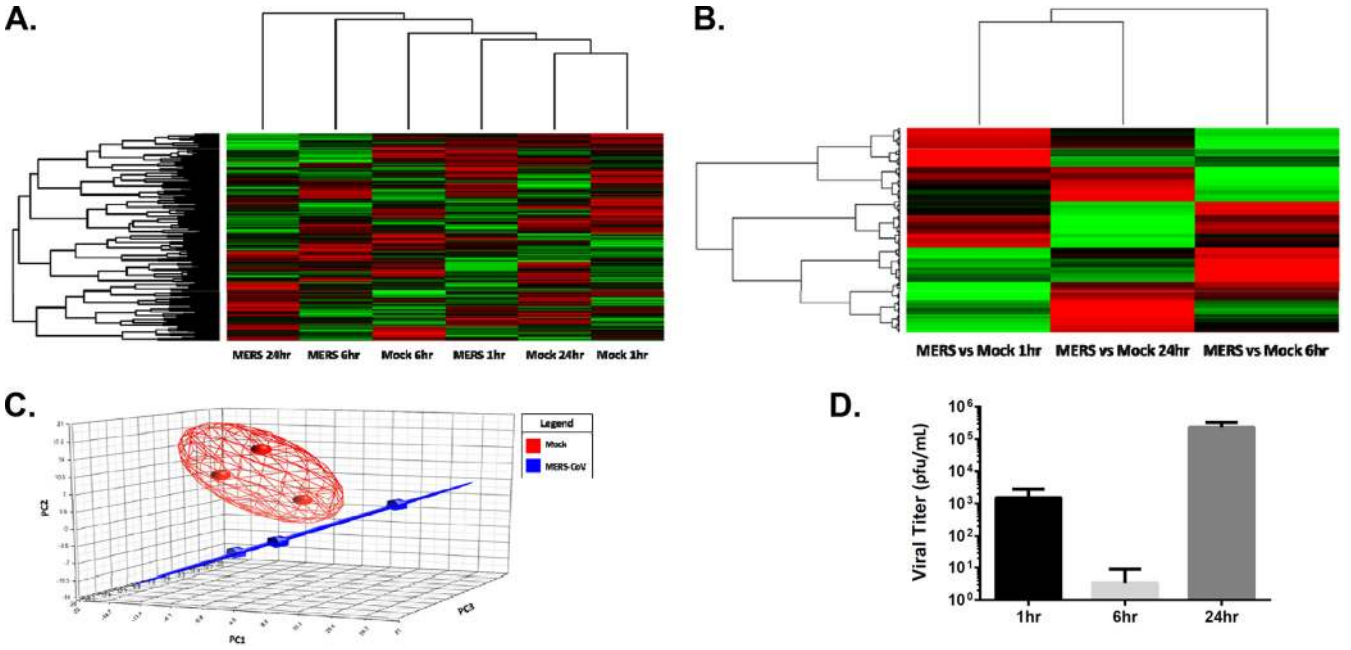

FIG 1 Heat maps and hierarchical clustering of host kinome responses to MERS-CoV infection. Peptide phosphorylation was assessed by densitometry. The results were scaled and normalized using GeneSpring (version 6.0) software. For hierarchical clustering, 1 − Pearson correlation coefficient was used as the distance metric and the McQuitty method was used as the linkage method. (A) Hierarchical clustering of the MERS-CoV-infected kinome data sets alongside the mock-infected control data sets. (B) Cluster analysis of the MERS-CoV-infected kinome data sets following background subtraction of the time-matched mock-infected control data sets. Spots demonstrating a significant differential phosphorylation between the MERS-CoV-infected and mock-infected control were compiled into a data set for each time point for comparative analysis. The lines at the top of the heat maps indicate the relative similarity between the conditions listed along the bottom edge of the heat maps. Line length indicates the degree of similarity, with shorter lines equating to stronger similarity. The lines on the left side of the heat maps indicate the relative similarity of the signal between the 300 individual peptide targets on the arrays. Red indicates increased phosphorylation; green indicates decreased phosphorylation. (C) Principal component analysis of the mock- and MERS-CoV-infected kinome data sets. (D) MERS-CoV titers from infected cells at each time point during the experiment.

response compared with that of the mock-infected samples at these time points (Fig. 1A). The results of clustering analysis of the kinome data following biological subtraction of the time-matched mock-infected kinome data sets from their MERS-CoV-infected counterparts are presented in Fig. 1B. Further, principal component analysis (PCA) of the kinome data for the mock- and MERS-CoV-infected samples demonstrated complete separation of the data sets into two individual clusters (Fig. 1C). Titration of cell culture supernatants from our kinome analysis by plaque assay also demonstrated that these cells were productively infected during the course of our analysis (Fig. 1D). It should be noted that the viral titers determined at 1 h p.i. represent the amount of virus remaining in the supernatant at this time point prior to washing of the cells.

Systems analysis of temporal kinome data. To gain biological insight into the molecular host response to MERS-CoV infection, we employed pathway overrepresentation analysis (ORA) with both the InnateDB and the IPA software suites. Pathway overrepresentation analysis with InnateDB was performed in an effort to identify specific signaling pathways that were modulated throughout the course of MERS-CoV infection. Analysis of the upregulated signaling pathways at all time points demonstrated that MERS-CoV infection modulated a broad range of cellular functions (see Table S1 in the supplemental material). Pathway ORA demonstrated that infection resulted in the modulation of host signaling pathways at 1 h p.i. Notably, multiple cell signaling pathways related to cell proliferation (cancer/carcinoma, growth factor signaling) and cell growth and differentiation (p53 effectors, Wnt signaling) were upregulated, while multiple proinflammatory signaling pathways (tumor necrosis factor alpha [TNF-α] and interleukin-1 [IL-1]) and innate immune response signaling pathways (Toll-like receptor [TLR] signaling) were downregulated at this time point. The signaling pathways identified to be modulated at 6 h and 24 h p.i. decreased in overall breadth and complexity compared to the breadth and complexity of the pathways identified to be modulated at the 1-h time point (see Table S1 in the supplemental material). In particular, by the 24-h time point the majority of upregulated signaling pathways were related to cell junctions (adherens junction and tight junction pathways) and Wnt-, transforming growth factor β-, or PI3K/AKT/mTOR-mediated signaling responses, with the concomitant downregulation of multiple innate immune response-related signaling pathways, including interleukin-, interferon- and TLR-related signaling pathways (see Table S1 in the supplemental material). We also observed specific trends within the signaling pathway data sets for each of the three time points. Pathways at the 1-h-p.i. time point had an overrepresentation of PI3K/AKT/mTOR pathway intermediates (including AKT1, mTOR, PDPK1, PIK3R1, PIK3R2, and RPS6KB1), ERK/MAPK pathway intermediates (including MAP2K1, MAPK3, and MAPK14), and NF-κB pathway intermediates (IKBKB, IKBKG, and NFKB1) within many of the signaling pathways identified. These trends also appeared to be largely conserved in both the 6-h-p.i. and 24-h-p.i. signaling pathway data, suggesting a potentially critical role for these pathways

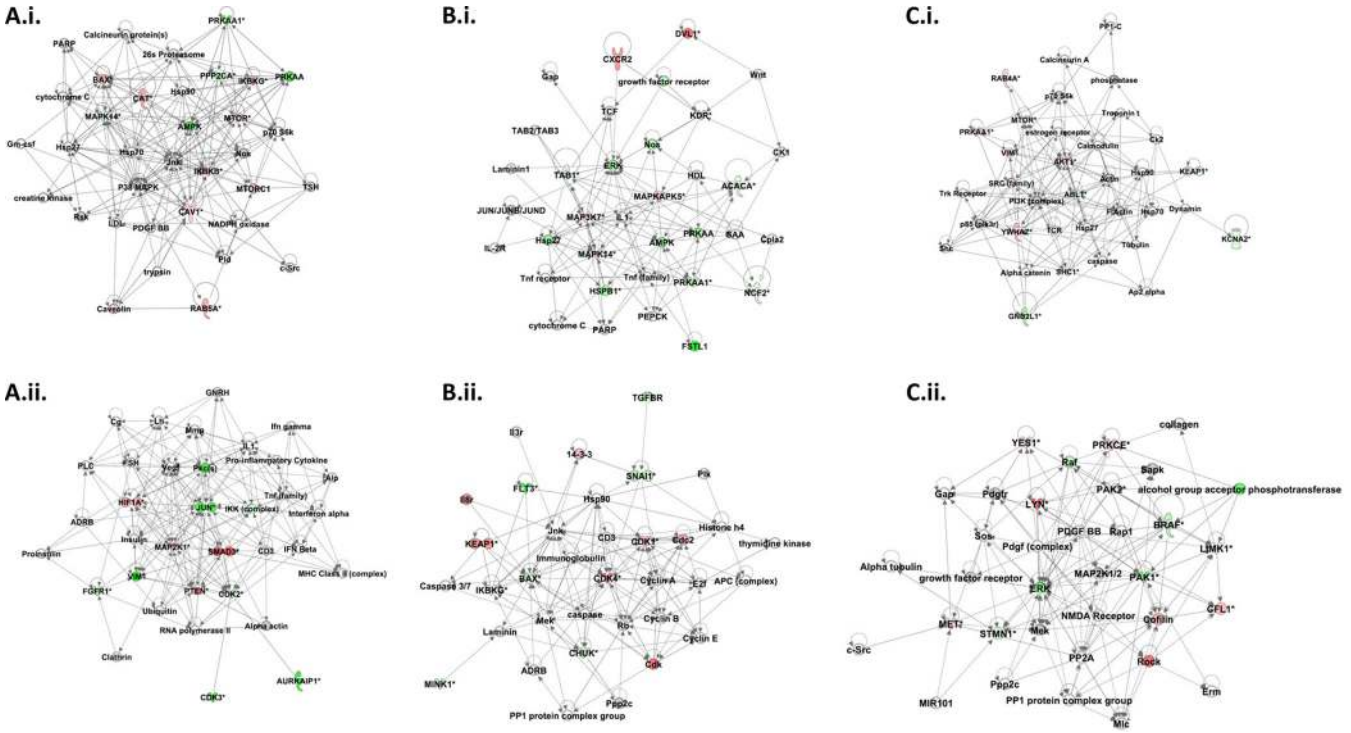

FIG 2 Functional network analysis of temporal kinome responses to MERS-CoV infection in Huh7 cells. Following PIIKA, kinome data sets comparing MERS-CoV-infected cells to mock-infected cells were uploaded to IPA for functional network analysis to identify kinases of potential pharmacological interest. The top two functional networks from each time point are presented. (A) Results at 1 h postinfection. (i) Network 1 (cell morphology, cellular function and maintenance, and carbohydrate metabolism); (ii) network 2 (embryonic development, organ development, organismal development). (B) Results at 6 h postinfection. (i) Network 1 (gene expression, RNA damage and repair, RNA posttranscriptional modification); (ii) network 2 (cell morphology, cellular function and maintenance, cell cycle). (C) Results at 24 h postinfection. (i) Network 1 (cancer, hematological disease, cell death and survival); (ii) network 2 (posttranslational modification, cell morphology, cellular assembly and organization). Red nodes, upregulation of phosphorylation; green nodes, downregulation of phosphorylation; PARP, procyclic acidic repetitive protein; CAT, chloramphenicol acetyltransferase; Cm-csf, granulocyte-macrophage colony-stimulating factor; LDL, low-density lipoprotein; PDGF BB, platelet-derived growth factor with two B chains; GNRH, gonadotropin-releasing hormone; PLC, phospholipase C; FSH, follicle-stimulating hormone; Vegf, vascular endothelial growth factor; IKK, IκB kinase; MHC, major histocompatibility complex; CDK2, cyclin-dependent kinase 2; TCF, T cell factor; HDL, high-density lipoprotein; IL2R, interleukin-2 receptor; PEPCK, phosphoenolpyruvate carboxykinase; FSTL1, follistatin-like 1; PP1C, phosphatase 1 catalytic subunit; TCR, T cell receptor; Pdgfr, platelet-derived growth factor receptor; NMDA, *N*-methyl-D-aspartate. Solid lines represent direct interactions between proteins, and dashed lines represent indirect interactions.

and intermediates in MERS-CoV infection. These signaling pathway trends were also confirmed by kinome analysis at 24 h p.i. in MRC5 cells, providing further evidence for a central role for PI3K/AKT/mTOR and ERK/MAPK signaling intermediates (data not shown).

Although these pathway identities were informative, we sought further insight into a broader biological role for these intermediates through functional network analysis (FNA) using the Ingenuity Pathway Analysis software suite. FNA does not limit genes or proteins to specific signaling pathways and instead provides predicted biological networks in which signaling intermediates are grouped on the basis of similarities in overall cellular responses and direct or indirect molecular interactions. The top two functional networks for each time point are presented in Fig. 2. FNA demonstrated that multiple intermediates within the ERK/MAPK signaling pathway (including ERK1 [MAP2K1], p38 [MAPK14], and MEK) and the PI3K/AKT/mTOR signaling pathway were conserved across multiple time points (Fig. 2A to C). It was also noted that ERK1/2 formed central nodes at both 1 h (Fig. 2Aii) and 24 h (Fig. 2Cii) postinfection, while AKT, PI3K, and mTOR formed a central core of the top network found at 24 h postinfection (Fig. 2Ci).

Comparative analysis of the significantly modulated phosphorylation events from our MERS-CoV kinome data by Venn analysis demonstrated that 14 kinases were conserved among data sets from the three p.i. time points (see Table S2 and Fig. S1A in the supplemental material). Interestingly, FNA of this peptide list resulted in multiple ERK/MAPK and PI3K/AKT/mTOR signaling pathway intermediates forming central components of the network, further suggesting that these pathways may be important components of the cellular events that accompany MERS-CoV infection (see Fig. S1B in the supplemental material). The associated biological functions of this network were identified to be cellular movement, cell death and survival, and the cell cycle.

Based on the trends discovered in our systems analysis of the kinome data, we chose to focus primarily on those signaling pathways or intermediates that were identified as being broadly conserved across our kinome analysis. Western blot analysis with Western blot arrays of protein phosphorylation demonstrated that MERS-CoV infection resulted in the modulation of ERK1/2 phosphorylation in a pattern that matched that found on the kinome arrays. The pattern of mTOR and AKT phosphorylation also matched that found from our kinome analysis. Further, the phosphorylation of downstream targets of mTOR, including S6

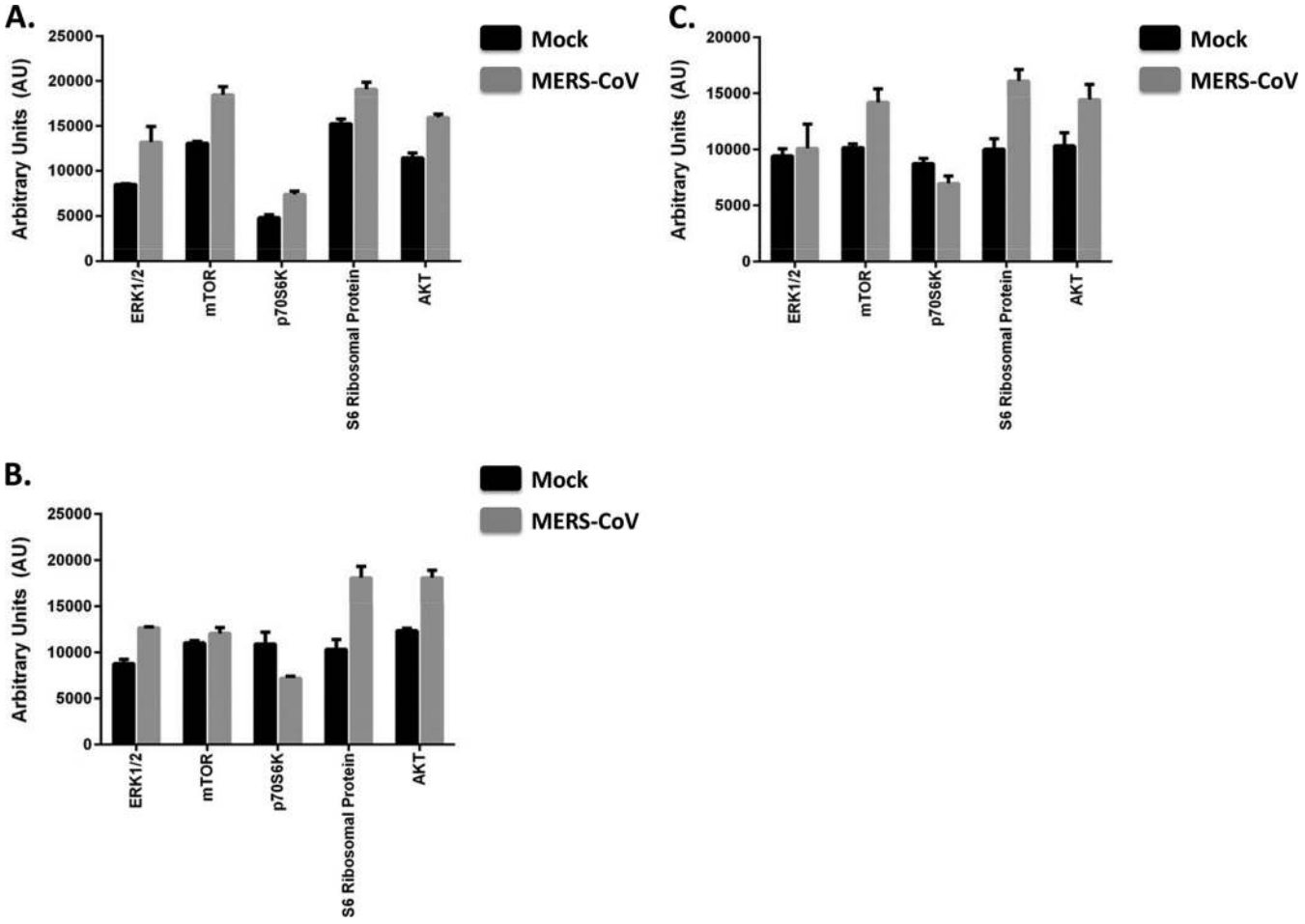

FIG 3 Western blot array analysis of select phosphorylation events in MERS-CoV-infected and mock-infected cells. Pixel intensities for selected spots on the array (in arbitrary units) are presented on the *y* axis. Results are presented as the mean ± SD. (A) Results at 1 h postinfection; (B) results at 6 h postinfection; (C) results at 24 h postinfection. The results represent those from one experiment (mean ± SD, $n = 3$), and the experiment was repeated twice.

ribosomal protein (S6RP) and p70S6 kinase (P70S6K), was also upregulated in a pattern that largely matched that of mTOR phosphorylation (Fig. 3A to C). Importantly, this type of phosphorylation analysis is largely qualitative rather than quantitative; however, the overall trends from our kinome analysis were in agreement with the trends found in our Western blot array analysis.

Kinase inhibitors targeting PI3K/AKT/mTOR and ERK/MAPK signaling inhibit MERS-CoV infection. Following our bioinformatics analysis of the kinome data, we sought further insight into the relationship between the host kinases or signaling networks that were overrepresented in our kinome data. As ERK/MAPK and PI3K/AKT/mTOR formed central components of multiple functional networks and signaling pathways within our analysis, we assessed the effect of selective inhibition of these kinases on MERS-CoV infection through a modified ELISA. Using our modified ELISA, we previously demonstrated that inhibition of MERS-CoV correlated with decreased viral titers through traditional plaque reduction assays (17). Thus, we chose to assess the effect of select kinase inhibitors targeting the PI3/AKT and ERK/MAPK pathways against MERS-CoV infection through this assay. We also selected inhibitors for specific kinases or signaling pathways identified from individual time points in our analysis (including protein kinase C [PKC]-, NF-κB-, nitric oxide synthase [NOS]-, and Src-mediated signaling responses). These host components either were found within the functional networks formed from our kinome data or were present within signaling pathways found in our pathway ORA. Importantly, at the highest concentration of kinase inhibitors tested (10 μM), all kinase inhibitors, with the exception of PKC-412 and Ro 31-8220 (20% and 23% cytotoxicity, respectively), had negligible (<10%) cytotoxic effects, as assessed by measurement of the level of lactate dehydrogenase, which is released during cell lysis (data not shown). For our analysis, we first examined the effects of kinase inhibitors when added 1 h prior to MERS-CoV infection *in vitro* using the same MOI used for the generation of the kinome data (MOI = 0.05). Inhibition of PI3K/AKT signaling with wortmannin resulted in 40% inhibition of MERS-CoV infection at the highest concentration tested, and inhibition decreased to 22% at submicromolar concentrations (Fig. 4A). In addition, treatment of cells with rapamycin, an inhibitor of mTOR, inhibited MERS-CoV infection by 61% at 10 μM and 24% at the lowest concentration tested (0.1 μM). Inhibitors for additional kinases that did not form critical components of signaling and/or the functional net-

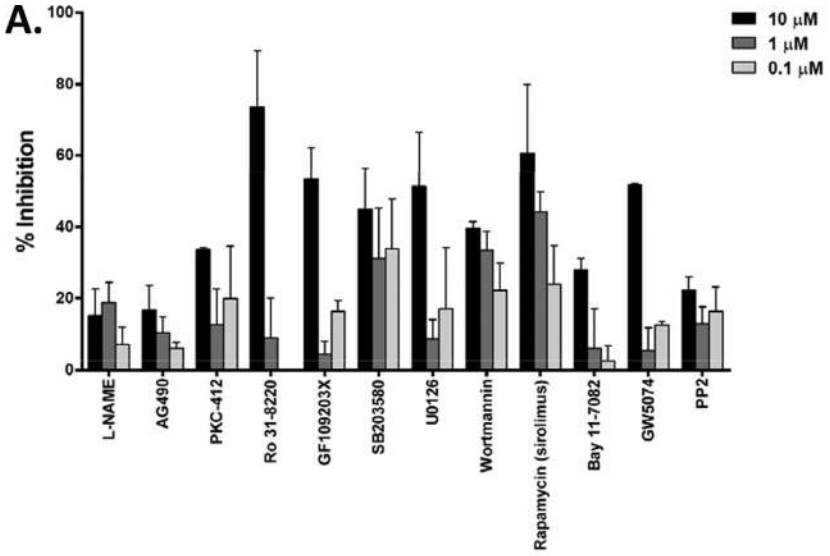

C.

Inhibitor	Cellular Target
L-NAME	nitric oxide synthase
AG490	EGFR; ERBB2
PKC-412	PKC
Ro 31-8220	PKC
GF109203X	PKC
SB203580	p38 MAPK
U0126	MEK1/2
Wortmannin	PI3K
Rapamycin	mTOR
Bay 11-7082	IKBα
GW5074	c-Raf1
PP2	Src

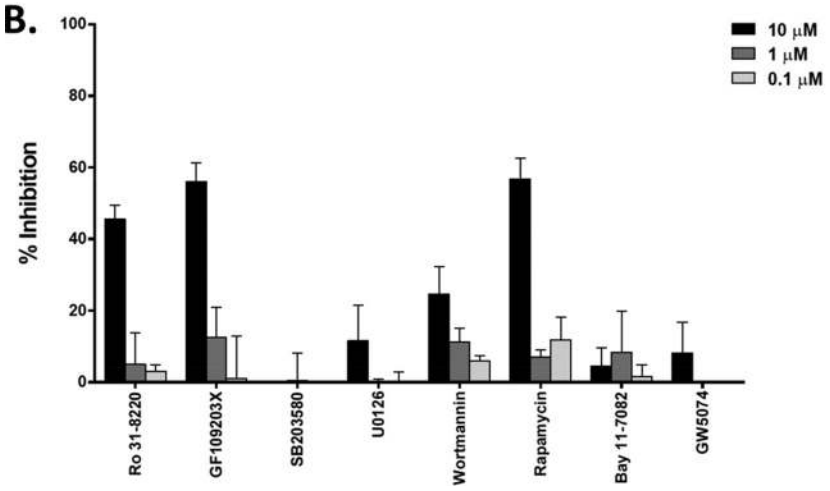

FIG 4 Inhibition of MERS-CoV infection by kinase inhibitors. Kinase inhibitors were added either preinfection (−1 h) or postinfection (+2 h) at the concentrations listed. Results are presented as the mean ± SD. (A) Preinfection addition of kinase inhibitors targeting signaling pathways/kinases identified from bioinformatics analysis of temporal kinome data; (B) postinfection addition of kinase inhibitors selected from panel A. The cytotoxicities for all compounds at the highest concentration tested (10 μM) were <10%, with the exception of those of PKC-412 and Ro 31-8220 (20% and 23%, respectively). (C) Kinase inhibitor targets from this analysis. The results represent those from three experimental repeats (mean ± SD, $n = 3$), with two technological repeats being performed in each experiment. EGFR, epidermal growth factor receptor.

work were also examined and had negligible effects on MERS-CoV infection. Taken together, these data provide further support for a role for the PI3K/AKT/mTOR signaling pathway during MERS-CoV infection.

Next, we examined the effects of ERK/MAPK pathway inhibitors. Pretreatment of cells with inhibitors of ERK/MAPK signaling resulted in the inhibition of MERS-CoV infection: SB203580 (p38 MAPK) and U0126 (MEK1/2) had similar inhibitory activities against MERS-CoV at 10 μM (45% and 51% inhibition, respectively). Pretreatment of cells with 10 μM GW5074, an inhibitor of Raf, a kinase that is involved in the ERK/MAPK signaling transduction cascade and was present in multiple signaling pathways identified from the kinome array data from 6 h and 24 h p.i., inhibited MERS-CoV by 52%. This also supported the findings from the analysis of the kinome data in regard to the modulation of ERK/MAPK signaling during MERS-CoV infection.

Inhibition of PKC prior to viral infection also resulted in inhibition of MERS-CoV (Fig. 3A). The PKC inhibitors PKC-412, GF109203X, and Ro 31-8220 inhibited MERS-CoV infection by 37%, 54%, and 74%, respectively, suggesting that PKC also plays an important role during infection. Inhibition of MERS-CoV infection by Ro 31-8220 and GF109203X was significantly greater than that by PKC-412 ($P < 0.1$). To examine the role for NF-κB signaling in MERS-CoV infection, cells were also pretreated with Bay 11-7082, an inhibitor of NF-κB DNA binding and tumor necrosis factor alpha (TNF-α)-induced IκBα phosphorylation that inhibited MERS-CoV infection by 28%. MERS-CoV was largely insensitive (<25% inhibition) to pretreatment of cells with inhibitors for Src (PP2), epidermal growth factor receptor (AG490), or NOS2 (L-NAME) (Fig. 4A).

To further assess the role for these kinases or signaling pathways in MERS-CoV infection, we selected inhibitors from our

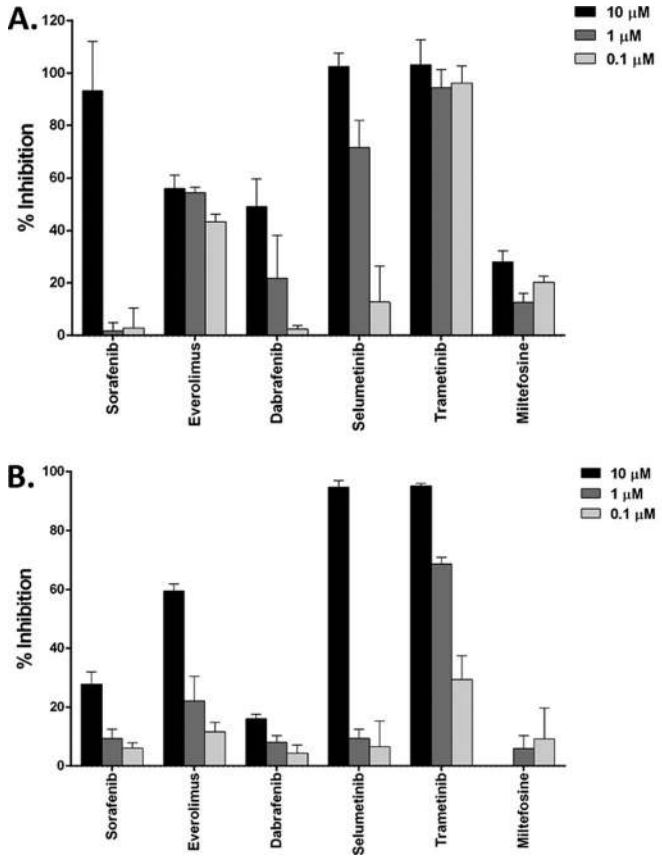

C.

Inhibitor	Cellular Target
Sorafenib	c-Raf; VEGFR; PDGFR
Everolimus	mTOR
Dabrafenib	B-Raf; C-Raf
Selumetinib	MEK1; ERK1/2
Trametinib	MEK1/2
Miltefosine	AKT

FIG 5 Inhibitory activity of FDA-licensed kinase inhibitors targeting ERK/MAPK or PI3K/AKT signaling added before or after MERS-CoV infection. Kinase inhibitors were added before (−1 h) or after (+2 h) MERS-CoV infection at the concentrations listed. Results are presented as the mean ± SD. (A) Preinfection addition of kinase inhibitors targeting signaling pathways/kinases identified from bioinformatics analysis of temporal kinome data. (B) Postinfection addition of kinase inhibitors. The cytotoxicities for all compounds tested were <10%. (C) Kinase inhibitor targets from this analysis. The results represent those from three experimental repeats (mean ± SD, $n = 3$), with two technological repeats performed in each experiment. For the pretreatment experiments, trametinib was significantly more inhibitory than selumetinib at 0.1 μM ($P < 0.05$). For the postaddition experiments, trametinib was significantly more inhibitory than selumetinib at 1 μM ($P < 0.005$). VEGFR, vascular endothelial growth factor receptor; PDGFR, platelet-derived growth factor receptor.

pretreatment experiments with inhibitory activities of ≥40% to examine the retention of these activities when added to the cells at 2 h p.i. Inhibitors that fit into this classification included inhibitors of PI3K (wortmannin), mTOR (rapamycin), MEK1/2 (U0126), PKC (Ro 31-8220, GF109203X), and c-Raf1 (GW5074). Addition of inhibitors from this subset to the cells at 2 h p.i. largely resulted in decreased inhibitory activity against MERS-CoV infection compared to that obtained with preinfection treatments. Postinfection treatment of cells with rapamycin (mTOR; 57%) had a significantly stronger inhibitory effect on infection than postinfection treatment of cells with wortmannin (PI3K; 25%), suggesting a more central role for mTOR than for PI3K during MERS-CoV infection ($P < 0.05$). Postinfection treatment of infected cells with Ro 31-8220 resulted in a modest conservation of inhibitory activity (46%) which was similar to that achieved with GF109203X (56%) and rapamycin (Fig. 3B).

As these analyses provided further support for the role of the ERK/MAPK and PI3K/AKT/mTOR signaling pathways initially identified from our kinome analysis, we postulated that licensed therapeutics targeting the same pathways would also have inhibitory activity against MERS-CoV infections. Here, we selected inhibitors targeting AKT (miltefosine), mTOR (everolimus), ERK/MAPK (selumetinib, trametinib), and Raf (dabrafenib, sorafenib). Cells were treated with inhibitors prior to (1 h) or following (2 h) MERS-CoV infection. For kinase inhibitors targeting the ERK/MAPK signal pathway, selumetinib (MEK1, ERK1/2) and trametinib (MEK1/2) had the strongest inhibitory activities of all the inhibitors tested (≥95%), including non-ERK/MAPK inhibitors, whether they were added prior to (−1 h; Fig. 5A) or following (+2 h; Fig. 5B) infection. Interestingly, trametinib demonstrated significantly stronger inhibitory activity against MERS-CoV than selumetinib at the lowest concentration tested when the inhibitors were added prior to infection ($P < 0.05$) or when a postinfection treatment concentration of 10 μM was used ($P < 0.05$). This suggests that these specific nodes of the ERK/MAPK signaling pathway (MEK1/2 and ERK1/2) may represent critical nodes of the biological responses of the host during MERS-CoV infection and may be the most logical targets for therapeutic intervention. We also examined inhibitors of Raf, a MAP3K found downstream of the Ras family of membrane GTPases, as Raf was found to be an intermediate in upregulated signaling pathways at all time points in our analysis and treatment of cells with GW5074 inhibited MERS-CoV infection (Fig. 3A). Pretreatment with sorafenib strongly inhibited MERS-COV infection (93%), provid-

ing further support for a role for the ERK/MAPK signaling pathway during viral infection. The inhibitory activity was reduced when sorafenib was added to cells at 2 h following infection (<30% inhibition at the highest concentration tested), suggesting that the role for Raf may be related primarily to processes early in the viral life cycle (viral entry, uptake or uncoating of virions) rather than viral replication processes. Dabrafenib, an inhibitor that also targets Raf, had reduced inhibitory activity against MERS-CoV compared to the activity of sorafenib (45%) when added to cells prior to MERS-CoV infection. As with sorafenib, the inhibitory activity of dabrafenib against MERS-CoV was largely negated when added to cells postinfection (Fig. 5B), providing further mechanistic evidence for a role for Raf primarily in early viral entry or postentry events.

From the perspective of PI3K/AKT/mTOR signaling, we also investigated licensed inhibitors that targeted AKT or mTOR. Everolimus, an inhibitor of mTOR, largely retained inhibitory activity against MERS-CoV whether it was added pre- or postinfection (56% and 59% inhibition, respectively, at 10 μM) (Fig. 5A). These results were very similar to those for rapamycin (sirolimus; Fig. 3A and B) and provide strong evidence for a critical role for mTOR in MERS-CoV infection. In contrast, miltefosine, an inhibitor of AKT approved for use for the treatment of leishmanial infection (33), had minimal inhibitory activity against MERS-CoV (28%) at the highest concentration tested when added preinfection. The activity was completely abrogated when added postinfection (Fig. 4B). As the inhibitory activity of everolimus was significantly greater than that of miltefosine at all concentrations tested ($P < 0.05$), this provided further support for a critical role for mTOR within the PI3K/AKT/mTOR signaling pathway in the exacerbation of MERS-COV infection. The results for selumetinib, trametinib, and everolimus were also confirmed by traditional plaque reduction assays. Huh7 cells were pretreated for 1 h with each of the three inhibitors (10 μM) and then infected at an MOI of 0.05, as in the initial kinome experiments. Following infection, cells were washed and then medium alone was added (see Fig. S2A in the supplemental material) or medium plus the inhibitor at the same concentration used in the preinfection treatments was added (see Fig. S2B in the supplemental material). A single preinfection addition of either selumetinib or trametinib resulted in a significant decrease in viral titers, and the readministration of inhibitor following infection (similar to the conditions for the cell-based ELISAs) resulted in significant inhibition of viral replication for all three inhibitors.

DISCUSSION

Concerns regarding the potential global implications of MERS-CoV as an emerging pathogen have been raised. As a result of this, there has been great interest in both increasing our understanding of the molecular pathogenesis associated with MERS-CoV infections and identifying potential therapeutic treatment options. Further, there is great interest in characterizing the molecular events that underlie host responses to MERS-CoV and the relation of these to disease pathogenesis and severity.

We and others have demonstrated the utility of kinome analysis for characterizing the molecular host response to viral infection through the identification of cell signaling networks or individual kinases that are uniquely modulated during these events (22, 34). Kinases are of critical importance to many biological processes and form an important mechanism for the regulation of these processes independent of changes in transcription or translation. As the dysregulation of cellular kinases has been implicated in numerous human malignancies (35), kinases have become an important target for the design and development of novel therapeutics (25, 26). There are currently 26 kinase inhibitors with FDA licensure and a continually increasing number at various stages of clinical development. It should also be appreciated that the escalating costs of moving a new drug from bench to bedside (estimated at more than $1 billion) have prompted calls for the investigation and potential repurposing of licensed therapeutics for alternative uses. Thus, kinome analysis provides a unique opportunity to characterize the molecular host response in the investigation of viral infections, including those caused by high-consequence pathogens. Here, we employed systems kinome analysis with peptide arrays to characterize the host response to MERS-CoV infection in Huh7 cells, a human hepatoma cell line that is highly permissive to MERS-CoV infection (27).

Our kinome analysis and subsequent pathway and functional network analyses demonstrated that MERS-CoV infection resulted in the selective modulation of the ERK/MAPK and PI3K/AKT/mTOR signaling responses throughout the course of infection. Recently, Josset et al. used an inverse genomic signature approach in their transcriptome analysis of MERS-CoV infection *in vitro* for the identification of potential drug targets (20). Our results complement those recently reported by Josset et al. in regard to the potential of kinase inhibitors to be novel treatments for MERS-CoV infection (20). The transcriptome analysis performed by the authors resulted in the prediction of two kinase inhibitors, LY294002 (PI3K) and SB203580 (p38 MAPK), to be potential modulators of MERS-CoV infection. Here, we have employed kinome analysis to provide critical data regarding the functional response of the host to viral infection through the analysis of the activation states of host kinases and cell signaling networks. Further, we have utilized this information for the logical prediction of host kinases that may serve as novel therapeutic targets for MERS-CoV infection. However, our analysis has expanded on these observations by providing functional evidence for the temporal roles of these signaling pathways in the host response during MERS-CoV infection (20).

We have demonstrated through systems-level analysis of our kinome data that multiple ERK/MAPK and PI3K/AKT/mTOR family members formed central components of functional networks and signaling pathways throughout the course of our investigation. In addition, ERK/MAPK and PI3K/AKT/mTOR signaling responses, including the functional network derived from the kinases that were conserved across all of the time points examined in our investigation, were overrepresented in our pathway and network analyses (see Fig. S1 in the supplemental material). The ERK/MAPK and PI3K/AKT/mTOR signaling networks are critical regulatory pathways for many cell regulatory responses, including cell proliferation and apoptosis, and have been demonstrated to be targeted by a broad range of viral pathogens (36–38). This would suggest that both ERK/MAPK and PI3K/AKT/mTOR signaling responses play important roles in the host response to MERS-CoV infection. Our kinome data and data from subsequent pathway and functional network analyses were corroborated by the phosphorylation patterns of specific members of these pathways obtained by Western blot array analysis. Further, the activation of mTOR-regulated intracellular kinases, including S6RP and p70S6K, lends further credence to our pathway and

functional network data. In addition to these findings, our analyses also suggested that PKC-mediated signaling also formed important components of the host response to MERS-CoV infection, as PKC formed components of both the functional and signaling pathway networks found in our investigation and the inhibition of PKC-mediated signaling responses resulted in decreased MERS-CoV infection whether it was added pre- or postinfection. As PKC can activate ERK/MAPK signaling (39), these results may provide additional information regarding the mechanism whereby MERS-CoV modulates ERK/MAPK signaling. A prior analysis of MERS-CoV infection also suggested that IFN responses and, in particular, those of IFN-β play important roles during the course of infection (17). Our analysis demonstrated that IFN-related signaling responses related to IFN signaling were found within the functional networks found at the 1-h-p.i. time point and, as well, were found in the downregulated signaling pathways at the 24-h-p.i. time point. These observations lend further credence to the growing evidence for a specific attenuation of IFN responses during MERS-CoV infection (17, 18, 40).

There has been considerable analysis of the therapeutic potential for host-targeted immunomodulatory agents in viral infections (20, 41, 42). Previous work has demonstrated that viruses modulate host cell signaling networks, including those involving PI3K/AKT/mTOR and ERK/MAPK. Human papillomavirus (HPV) is able to maintain an activated AKT, resulting in activated mTORC1, and it has been postulated that this may be required for the initiation of viral replication (43). A similar requirement for activated PI3K/AKT/mTOR signaling in viral replication has also been demonstrated for myxoma virus (44). Qin et al. have also demonstrated that herpes simplex virus 1 infection stimulated both the PI3K/AKT and ERK/MAPK signaling pathways (45), and the role of ERK/MAPK signaling modulation in viral infection has also been noted for reovirus (46), rabies virus (47), and hepatitis B virus (48), among others. We demonstrated that multiple licensed kinase inhibitors targeting the ERK/MAPK or PI3K/AKT/mTOR signaling pathway inhibited MERS-CoV infection *in vitro* when added prior to or following viral infection. Inhibitors of MEK1/2 (trametinib) and/or ERK1/2 (selumetinib) had the strongest and most conserved inhibitory activities, suggesting that MEK1/2 and ERK1/2 may have unique capabilities as stand-alone or combinatorial therapies for MERS-CoV infections. Further, across all time points, both ERK/MAPK intermediates were represented in signaling pathways or functional networks that were derived from our kinome analysis. These analyses also suggested that mTOR was highly overrepresented within our kinome data. Inhibitors of mTOR (rapamycin and everolimus) had reduced inhibitory activities against MERS-CoV compared to the activities of trametinib and selumetinib. However, the conservation of these activities following treatment pre- or postinfection also suggests that mTOR plays a critical role in MERS-CoV infections beyond viral entry. Although our kinome data suggested that PI3K could be an attractive therapeutic target for MERS-CoV and treatment of cells with wortmannin, a selective PI3K inhibitor, inhibited MERS-CoV infection, the administration of miltefosine (an AKT inhibitor licensed for use as an antileishmanial agent [33]) had minimal inhibitory activity in our analysis. These results suggest that in addition to ERK/MAPK intermediates, as targeted by trametinib and selumetinib, mTOR may also be a logical therapeutic target for MERS-CoV infections. These results were further validated by the significant reduction in viral titers demonstrated by a plaque reduction assay when cells were treated for only 1 h prior to infection (trametinib and selumetinib) or when inhibitors were replenished following infection (trametinib, selumetinib, and everolimus). The specific mechanism(s) of inhibition for these inhibitors remains to be determined. Though it is postulated that this inhibitory effect is mitigated through the direct inactivation of the primary targets of these inhibitors, it is appreciated that many licensed kinase inhibitors have off-site targets that could contribute to the overall antiviral activities reported here. Specific inhibition of intermediates from the ERK/MAPK and PI3K/AKT/mTOR signaling pathways through approaches that use, for example, small interfering RNA knockdown or gene knockout will help shed light on this question. Although it is tempting to speculate that these compounds may have the potential to be used for the treatment of MERS-CoV infections in the future, their use will require additional investigations of their associated pharmacokinetics and the correlation of these with the levels required for antiviral activity *in vivo*. Future investigations will expand on these findings to determine the precise mechanism of action for these inhibitors in the MERS-CoV viral life cycle (i.e., inhibition of viral replication, viral assembly, or viral egress).

Using kinome analysis, we have demonstrated that MERS-CoV infection resulted in the selective modulation of the ERK/MAPK and PI3K/AKT/mTOR signaling responses in the host and confirmed this through biological validation experiments with kinase inhibitors. Further, we have also demonstrated the utility of temporal kinome analysis for characterizing host responses to infection and for the subsequent selection of therapeutics that may provide resolution of the infection. Taken together, we provide critical information regarding the molecular host response to MERS-CoV infection and evidence for the potential of kinase inhibitor therapeutics with preexisting licensure to be novel strategies for the treatment of MERS-CoV infections.

ACKNOWLEDGMENTS

This study was supported in part by the NIAID Division of Intramural Research.

B.J.H., J.D., and J.H.K. performed this work as employees of Tunnell Consulting, Inc., and D.T. and S.M. performed this work as employees of MRI Global. Tunnell Consulting, Inc., and MRI Global are subcontractors to Battelle Memorial Institute. J.K., B.O., and M.H. performed this work as employees of Battelle Memorial Institute. All work was performed under the Battelle Memorial Institute prime contract with NIAID (contract no. HHSN272200700016I).

The content of this publication does not necessarily reflect the views or policies of the U.S. Department of Health and Human Services or of the institutions and companies affiliated with the authors.

REFERENCES

1. **Zaki AM, van Boheemen S, Bestebroer TM, Osterhaus AD, Fouchier RA.** 2012. Isolation of a novel coronavirus from a man with pneumonia in Saudi Arabia. N Engl J Med **367:**1814–1820. http://dx.doi.org/10.1056/NEJMoa1211721.
2. **Raj VS, Osterhaus AD, Fouchier RA, Haagmans BL.** 2014. MERS: emergence of a novel human coronavirus. Curr Opin Virol **5:**58–62. http://dx.doi.org/10.1016/j.coviro.2014.01.010.
3. **Bialek SR, Allen D, Alvarado-Ramy F, Arthur R, Balajee A, Bell D, Best S, Blackmore C, Breakwell L, Cannons A, Brown C, Cetron M, Chea N, Chommanard C, Cohen N, Conover C, Crespo A, Creviston J, Curns AT, Dahl R, Dearth S, DeMaria A, Echols F, Erdman DD, Feikin D, Frias M, Gerber SI, Gulati R, Hale C, Haynes LM, Heberlein-Larson L, Holton K, Ijaz K, Kapoor M, Kohl K, Kuhar DT, Kumar AM, Kundich M, Lippold S, Liu L, Lovchik JC, Madoff L, Martell S, Matthews S,**

Moore J, Murray LR, Onofrey S, Pallansch MA, Pesik N, Pham H, et al. 2014. First confirmed cases of Middle East respiratory syndrome coronavirus (MERS-CoV) infection in the United States, updated information on the epidemiology of MERS-CoV infection, and guidance for the public, clinicians, and public health authorities—May 2014. MMWR Morb Mortal Wkly Rep **63:**431–436.

4. **Peiris JS, Yuen KY, Osterhaus AD, Stohr K.** 2003. The severe acute respiratory syndrome. N Engl J Med **349:**2431–2441. http://dx.doi.org/10.1056/NEJMra032498.
5. **Pyrc K, Sims AC, Dijkman R, Jebbink M, Long C, Deming D, Donaldson E, Vabret A, Baric R, van der Hoek L, Pickles R.** 2010. Culturing the unculturable: human coronavirus HKU1 infects, replicates, and produces progeny virions in human ciliated airway epithelial cell cultures. J Virol **84:**11255–11263. http://dx.doi.org/10.1128/JVI.00947-10.
6. **Lau SK, Li KS, Tsang AK, Lam CS, Ahmed S, Chen H, Chan KH, Woo PC, Yuen KY.** 2013. Genetic characterization of *Betacoronavirus* lineage C viruses in bats reveals marked sequence divergence in the spike protein of *Pipistrellus* bat coronavirus HKU5 in Japanese pipistrelle: implications for the origin of the novel Middle East respiratory syndrome coronavirus. J Virol **87:**8638–8650. http://dx.doi.org/10.1128/JVI.01055-13.
7. **van Boheemen S, de Graaf M, Lauber C, Bestebroer TM, Raj VS, Zaki AM, Osterhaus AD, Haagmans BL, Gorbalenya AE, Snijder EJ, Fouchier RA.** 2012. Genomic characterization of a newly discovered coronavirus associated with acute respiratory distress syndrome in humans. mBio **3**(6):e00473-12. http://dx.doi.org/10.1128/mBio.00473-12.
8. **Coleman CM, Frieman MB.** 2013. Emergence of the Middle East respiratory syndrome coronavirus. PLoS Pathog **9:**e1003595. http://dx.doi.org/10.1371/journal.ppat.1003595.
9. **Alagaili AN, Briese T, Mishra N, Kapoor V, Sameroff SC, de Wit E, Munster VJ, Hensley LE, Zalmout IS, Kapoor A, Epstein JH, Karesh WB, Daszak P, Mohammed OB, Lipkin WI.** 2014. Middle East respiratory syndrome coronavirus infection in dromedary camels in Saudi Arabia. mBio 5(2):e00884-14. http://dx.doi.org/10.1128/mBio.00884-14.
10. **Ferguson NM, Van Kerkhove MD.** 2014. Identification of MERS-CoV in dromedary camels. Lancet Infect Dis **14:**93–94. http://dx.doi.org/10.1016/S1473-3099(13)70691-1.
11. **Zumla AI, Memish ZA.** 2014. Middle East respiratory syndrome coronavirus: epidemic potential or a storm in a teacup? Eur Respir J **43:**1243–1248. http://dx.doi.org/10.1183/09031936.00227213.
12. **Bermingham A, Chand MA, Brown CS, Aarons E, Tong C, Langrish C, Hoschler K, Brown K, Galiano M, Myers R, Pebody RG, Green HK, Boddington NL, Gopal R, Price N, Newsholme W, Drosten C, Fouchier RA, Zambon M.** 2012. Severe respiratory illness caused by a novel coronavirus, in a patient transferred to the United Kingdom from the Middle East, September 2012. Euro Surveill **17**(40):pii=20290. http://www.eurosurveillance.org/ViewArticle.aspx?ArticleId=20290.
13. **Geng H, Tan W.** 2013. A novel human coronavirus: Middle East respiratory syndrome human coronavirus. Sci China Life Sci **56:**683–687. http://dx.doi.org/10.1007/s11427-013-4519-8.
14. **Al-Tawfiq JA, Memish ZA.** 2014. What are our pharmacotherapeutic options for MERS-CoV? Expert Rev Clin Pharmacol **7:**235–238. http://dx.doi.org/10.1586/17512433.2014.890515.
15. **Zielecki F, Weber M, Eickmann M, Spiegelberg L, Zaki AM, Matrosovich M, Becker S, Weber F.** 2013. Human cell tropism and innate immune system interactions of human respiratory coronavirus EMC compared to those of severe acute respiratory syndrome coronavirus. J Virol **87:**5300–5304. http://dx.doi.org/10.1128/JVI.03496-12.
16. **Kindler E, Jonsdottir HR, Muth D, Hamming OJ, Hartmann R, Rodriguez R, Geffers R, Fouchier RA, Drosten C, Muller MA, Dijkman R, Thiel V.** 2013. Efficient replication of the novel human betacoronavirus EMC on primary human epithelium highlights its zoonotic potential. mBio **4**(1):e00611-12. http://dx.doi.org/10.1128/mBio.00611-12.
17. **Hart BJ, Dyall J, Postnikova E, Zhou H, Kindrachuk J, Johnson RF, Olinger GG, Jr, Frieman MB, Holbrook MR, Jahrling PB, Hensley L.** 2014. Interferon-beta and mycophenolic acid are potent inhibitors of Middle East respiratory syndrome coronavirus in cell-based assays. J Gen Virol **95:**571–577. http://dx.doi.org/10.1099/vir.0.061911-0.
18. **Chan JF, Chan KH, Kao RY, To KK, Zheng BJ, Li CP, Li PT, Dai J, Mok FK, Chen H, Hayden FG, Yuen KY.** 2013. Broad-spectrum antivirals for the emerging Middle East respiratory syndrome coronavirus. J Infect **67:**606–616. http://dx.doi.org/10.1016/j.jinf.2013.09.029.
19. **Falzarano D, de Wit E, Martellaro C, Callison J, Munster VJ, Feldmann H.** 2013. Inhibition of novel β coronavirus replication by a combination of interferon-α2b and ribavirin. Sci Rep **3:**1686. http://dx.doi.org/10.1038/srep01686.
20. **Josset L, Menachery VD, Gralinski LE, Agnihothram S, Sova P, Carter VS, Yount BL, Graham RL, Baric RS, Katze MG.** 2013. Cell host response to infection with novel human coronavirus EMC predicts potential antivirals and important differences with SARS coronavirus. mBio **4**(3):e00165-13. http://dx.doi.org/10.1128/mBio.00165-13.
21. **Clarke P, Leser JS, Bowen RA, Tyler KL.** 2014. Virus-induced transcriptional changes in the brain include the differential expression of genes associated with interferon, apoptosis, interleukin 17 receptor A, and glutamate signaling as well as flavivirus-specific upregulation of tRNA synthetases. mBio **5**(2):e00902-14. http://dx.doi.org/10.1128/mBio.00902-14.
22. **Kindrachuk J, Arsenault R, Kusalik A, Kindrachuk KN, Trost B, Napper S, Jahrling PB, Blaney JE.** 2012. Systems kinomics demonstrates Congo Basin monkeypox virus infection selectively modulates host cell signaling responses as compared to West African monkeypox virus. Mol Cell Proteomics **11:**M111.015701. http://dx.doi.org/10.1074/mcp.M111.015701.
23. **Maattanen P, Trost B, Scruten E, Potter A, Kusalik A, Griebel P, Napper S.** 2013. Divergent immune responses to Mycobacterium avium subsp. paratuberculosis infection correlate with kinome responses at the site of intestinal infection. Infect Immun **81:**2861–2872. http://dx.doi.org/10.1128/IAI.00339-13.
24. **Mulongo M, Prysliak T, Scruten E, Napper S, Perez-Casal J.** 2014. In vitro infection of bovine monocytes with Mycoplasma bovis delays apoptosis and suppresses production of gamma interferon and tumor necrosis factor alpha but not interleukin-10. Infect Immun **82:**62–71. http://dx.doi.org/10.1128/IAI.00961-13.
25. **Cohen P.** 2002. Protein kinases—the major drug targets of the twenty-first century? Nat Rev Drug Discov **1:**309–315. http://dx.doi.org/10.1038/nrd773.
26. **Hopkins AL, Groom CR.** 2002. The druggable genome. Nat Rev Drug Discov **1:**727–730. http://dx.doi.org/10.1038/nrd892.
27. **de Wilde AH, Raj VS, Oudshoorn D, Bestebroer TM, van Nieuwkoop S, Limpens RW, Posthuma CC, van der Meer Y, Barcena M, Haagmans BL, Snijder EJ, van den Hoogen BG.** 2013. MERS-coronavirus replication induces severe in vitro cytopathology and is strongly inhibited by cyclosporin A or interferon-alpha treatment. J Gen Virol **94:**1749–1760. http://dx.doi.org/10.1099/vir.0.052910-0.
28. **de Wit E, Rasmussen AL, Falzarano D, Bushmaker T, Feldmann F, Brining DL, Fischer ER, Martellaro C, Okumura A, Chang J, Scott D, Benecke AG, Katze MG, Feldmann H, Munster VJ.** 2013. Middle East respiratory syndrome coronavirus (MERS-CoV) causes transient lower respiratory tract infection in rhesus macaques. Proc Natl Acad Sci U S A **110:**16598–16603. http://dx.doi.org/10.1073/pnas.1310744110.
29. **Li Y, Arsenault RJ, Trost B, Slind J, Griebel PJ, Napper S, Kusalik A.** 2012. A systematic approach for analysis of peptide array kinome data. Sci Signal **5:**pl2. http://dx.doi.org/10.1126/scisignal.2002429.
30. **Trost B, Kindrachuk J, Maattanen P, Napper S, Kusalik A.** 2013. PIIKA 2: an expanded, web-based platform for analysis of kinome microarray data. PLoS One **8:**e80837. http://dx.doi.org/10.1371/journal.pone.0080837.
31. **Lynn DJ, Winsor GL, Chan C, Richard N, Laird MR, Barsky A, Gardy JL, Roche FM, Chan TH, Shah N, Lo R, Naseer M, Que J, Yau M, Acab M, Tulpan D, Whiteside MD, Chikatamarla A, Mah B, Munzner T, Hokamp K, Hancock RE, Brinkman FS.** 2008. InnateDB: facilitating systems-level analyses of the mammalian innate immune response. Mol Syst Biol **4:**218. http://dx.doi.org/10.1038/msb.2008.55.
32. **Schneider CA, Rasband WS, Eliceiri KW.** 2012. NIH Image to ImageJ: 25 years of image analysis. Nat Methods **9:**671–675. http://dx.doi.org/10.1038/nmeth.2089.
33. **Dorlo TP, Balasegaram M, Beijnen JH, de Vries PJ.** 2012. Miltefosine: a review of its pharmacology and therapeutic efficacy in the treatment of leishmaniasis. J Antimicrob Chemother **67:**2576–2597. http://dx.doi.org/10.1093/jac/dks275.
34. **Bowick GC, Fennewald SM, Scott EP, Zhang L, Elsom BL, Aronson JF, Spratt HM, Luxon BA, Gorenstein DG, Herzog NK.** 2007. Identification of differentially activated cell-signaling networks associated with pichinde virus pathogenesis by using systems kinomics. J Virol **81:**1923–1933. http://dx.doi.org/10.1128/JVI.02199-06.
35. **Knuutila S, Bjorkqvist AM, Autio K, Tarkkanen M, Wolf M, Monni O, Szymanska J, Larramendy ML, Tapper J, Pere H, El-Rifai W, Hemmer S, Wasenius VM, Vidgren V, Zhu Y.** 1998. DNA copy number amplifications in human neoplasms: review of comparative genomic hybridization studies. Am J Pathol **152:**1107–1123.

36. **Ji WT, Liu HJ.** 2008. PI3K-Akt signaling and viral infection. Recent Pat Biotechnol **2:**218–226. http://dx.doi.org/10.2174/187220808786241042.
37. **Ehrhardt C, Ludwig S.** 2009. A new player in a deadly game: influenza viruses and the PI3K/Akt signalling pathway. Cell Microbiol **11:**863–871. http://dx.doi.org/10.1111/j.1462-5822.2009.01309.x.
38. **Pleschka S.** 2008. RNA viruses and the mitogenic Raf/MEK/ERK signal transduction cascade. Biol Chem **389:**1273–1282. http://dx.doi.org/10.1515/BC.2008.145.
39. **Ueda Y, Hirai S, Osada S, Suzuki A, Mizuno K, Ohno S.** 1996. Protein kinase C activates the MEK-ERK pathway in a manner independent of Ras and dependent on Raf. J Biol Chem **271:**23512–23519. http://dx.doi.org/10.1074/jbc.271.38.23512.
40. **Falzarano D, de Wit E, Rasmussen AL, Feldmann F, Okumura A, Scott DP, Brining D, Bushmaker T, Martellaro C, Baseler L, Benecke AG, Katze MG, Munster VJ, Feldmann H.** 2013. Treatment with interferon-alpha2b and ribavirin improves outcome in MERS-CoV-infected rhesus macaques. Nat Med **19:**1313–1317. http://dx.doi.org/10.1038/nm.3362.
41. **Ludwig S.** 2011. Disruption of virus-host cell interactions and cell signaling pathways as an anti-viral approach against influenza virus infections. Biol Chem **392:**837–847. http://dx.doi.org/10.1515/BC.2011.121.
42. **Tisoncik JR, Korth MJ, Simmons CP, Farrar J, Martin TR, Katze MG.** 2012. Into the eye of the cytokine storm. Microbiol Mol Biol Rev **76:**16–32. http://dx.doi.org/10.1128/MMBR.05015-11.
43. **Buchkovich NJ, Yu Y, Zampieri CA, Alwine JC.** 2008. The TORrid affairs of viruses: effects of mammalian DNA viruses on the PI3K-Akt-mTOR signalling pathway. Nat Rev Microbiol **6:**266–275. http://dx.doi.org/10.1038/nrmicro1855.
44. **Wang G, Barrett JW, Stanford M, Werden SJ, Johnston JB, Gao X, Sun M, Cheng JQ, McFadden G.** 2006. Infection of human cancer cells with myxoma virus requires Akt activation via interaction with a viral ankyrin-repeat host range factor. Proc Natl Acad Sci U S A **103:**4640–4645. http://dx.doi.org/10.1073/pnas.0509341103.
45. **Qin D, Feng N, Fan W, Ma X, Yan Q, Lv Z, Zeng Y, Zhu J, Lu C.** 2011. Activation of PI3K/AKT and ERK MAPK signal pathways is required for the induction of lytic cycle replication of Kaposi's sarcoma-associated herpesvirus by herpes simplex virus type 1. BMC Microbiol **11:**240. http://dx.doi.org/10.1186/1471-2180-11-240.
46. **Norman KL, Hirasawa K, Yang AD, Shields MA, Lee PW.** 2004. Reovirus oncolysis: the Ras/RalGEF/p38 pathway dictates host cell permissiveness to reovirus infection. Proc Natl Acad Sci U S A **101:**11099–11104. http://dx.doi.org/10.1073/pnas.0404310101.
47. **Nakamichi K, Inoue S, Takasaki T, Morimoto K, Kurane I.** 2004. Rabies virus stimulates nitric oxide production and CXC chemokine ligand 10 expression in macrophages through activation of extracellular signal-regulated kinases 1 and 2. J Virol **78:**9376–9388. http://dx.doi.org/10.1128/JVI.78.17.9376-9388.2004.
48. **Chung TW, Lee YC, Kim CH.** 2004. Hepatitis B viral HBx induces matrix metalloproteinase-9 gene expression through activation of ERK and PI-3K/AKT pathways: involvement of invasive potential. FASEB J **18:**1123–1125. http://dx.doi.org/10.1096/fj.03-1429fje.